

# Ginsenoside Rg3 attenuates hepatoma VEGF overexpression after hepatic artery embolization in an orthotopic transplantation hepatocellular carcinoma rat model

Bo Zhou  
Jianhua Wang  
Zhiping Yan

Department of Interventional Radiology, Zhongshan Hospital, Shanghai Medical College, Fudan University, People's Republic of China

**Background:** Hypoxia-induced vascular endothelial growth factor (VEGF) upregulation and angiogenesis following treatment of hepatocellular carcinoma (HCC) with transarterial embolization (TAE) or transarterial chemoembolization (TACE) may be mediated by ginsenoside Rg3, an anti-angiogenic saponin extracted from ginseng.

**Objective:** To access the synergistic action of Rg3 and TAE treatment on HCC by VEGF and its receptor expressions decreasing in a rat model of HCC.

**Methods:** An orthotopic transplantation HCC model was established in Buffalo rats. HCC rats were treated with hepatic artery infusions of normal saline or iodized oil (0.1 mL) with or without Rg3 (1 mg/kg) (each n=15 in control, Rg3, TAE, and TAE + Rg3 groups). At 1, 2, 4, and 8 weeks, performance status (body weight), tumor progression (longest tumor diameter), metastasis rate, microvessel density (MVD), and overall survival rate were assessed. Additionally, cluster of differentiation 31 (CD31), VEGF, VEGF receptor 2 (VEGF-R2) and VEGF-R2 phosphorylation levels were assessed by immunohistochemistry, enzyme-linked immunosorbent assay (ELISA), and Western blot.

**Results:** Combined Rg3 and TAE treatment reduced tumor progression, body weight loss, angiogenesis, and metastasis rate, and led to better overall survival in the HCC rat model. ELISA results showing VEGF expression in the control, Rg3, TAE, and TAE + Rg3 groups at 4 weeks following treatment were  $132.6 \pm 2.38$ ,  $37.9 \pm 0.8$ ,  $87.4 \pm 0.7$ , and  $45.3 \pm 0.4$  pg/mL, respectively. Combined Rg3 and TAE reduced the protein expression of CD31 and VEGF-R2 phosphorylation, compared with those in the TAE group at 4 weeks of treatment.

**Conclusion:** Combined Rg3 and TAE treatment limited metastasis and promoted survival by downregulating VEGF overexpression in HCC tumors. Thus, this treatment may have potential clinical implications for HCC patients undergoing TAE or TACE.

**Keywords:** ginsenoside Rg3, vascular endothelial growth factor, hepatocellular carcinoma, angiogenesis, hypoxia

## Introduction

Combined anti-angiogenic agents and local treatments, including embolization of hepatic artery branches using transarterial embolization (TAE) or transarterial chemoembolization (TACE), have been proposed for treatment of hepatocellular carcinoma (HCC), a common malignancy affecting over 748,000 new patients each year.<sup>1,2</sup> Currently, TAE or TACE can improve survival time for inoperable patients;<sup>3</sup> however, recurrence and metastasis still remain common in these patients after treatment due to incomplete removal of tumor tissues supplied by the hepatic portal system.<sup>4</sup> In Europe

Correspondence: Bo Zhou; Jianhua Wang  
Department of Interventional Radiology, Zhongshan Hospital, Shanghai Medical College, Fudan University, 180 Fenglin Road, Shanghai 200032, People's Republic of China  
Tel +86 136 2160 4953  
Fax +86 21 6408 5875  
Email bonheuzhou@hotmail.com; wangjianhua2013@sina.cn

and America, HCC incidence remains relatively low (1–10 per 100,000); however, southeast Asia, sub-Saharan western and eastern Africa, and the People's Republic of China report HCC in more than 20 of every 100,000 people, with up to 55% of these cases reported in the People's Republic of China.<sup>5,6</sup> Thus, there is an urgent need for improved HCC treatments, particularly in these regions.

TAE and TACE are designed to promote necrosis in hypervascular HCC tumor tissues by blocking the arterial supply to malignant tissues; however, the resultant period of induced hypoxia may also upregulate angiogenic factors, such as insulin-like growth factor 2 (IGF-2) and vascular endothelial growth factor (VEGF), thereby promoting proliferation and metastasis of remaining tumor cells supplied by the portal system.<sup>1</sup> Even before treatment, VEGF upregulation of up to seven times greater than normal values has been reported in endothelial cells in carcinoma areas.<sup>7</sup> Following TAE or TACE treatment, however, a zone of distinct hypoxic stress forms between the necrotic central area and surviving margin of treated tumors, which is central to temporary overexpression of growth and angiogenic factors as well as Rac activation, which is also associated with VEGF overexpression and subsequent metastasis.<sup>1</sup> Thus, the usefulness of TAE and TACE treatment is limited by the high incidence of tumor recurrence and metastasis.<sup>8,9</sup>

Anti-angiogenic agents such as sorafenib have opened the door for more effective prevention of metastasis and recurrence following local treatment of HCC and other cancers. Sorafenib is a multi-target VEGF and Raf kinase inhibitor that can extend the survival of advanced HCC patients, but its application is limited by high cost, frequent adverse events, and unsatisfactory efficacy.<sup>10</sup> Recently, ginsenoside Rg3, an anti-angiogenic saponin extracted from red ginseng, has been reported to down-regulate hypoxia-induced VEGF expression in human cancer cells.<sup>11,12</sup> Thus, a combination of ginsenoside Rg3 and TAE or TACE may potentially be able to limit hypoxia-induced VEGF expression as well as potentially inhibit expression of other factors related to angiogenesis and metastasis in HCC.

The ability of combined ginsenoside Rg3 and TAE treatment to attenuate hypoxia-induced VEGF overexpression in an orthotopic transplantation HCC rat model was investigated, thereby providing preliminary evidence for the benefits of this treatment.

## Materials and methods

### Animals

Male and female Buffalo rats were obtained from Charles River Laboratories (Wilmington, MA, USA) and maintained

in the animal care facility of the Zhongshan Hospital (Shanghai, People's Republic of China). All animals were housed under specific pathogen free (SPF) conditions with ad libitum access to sterile food and water and a 12/12-hour light/dark cycle. The experimental protocol and all animal treatments were approved by the Ethics Committee of Zhongshan Hospital, Fudan University Shanghai Medical College, Shanghai, People's Republic of China.

### Cell culture and establishment of subcutaneously heterotopic transplantation HCC model in the rats

Syngeneic hepatoma cell line McA-RH7777 (American Type Culture Collection [ATCC] No CRL 1601, Rockville, MD, USA) was cultured in Dulbecco's Modified Eagle's Medium (DMEM) with 4,500 g/L glucose (Gibco®/Thermo Fisher Scientific, Grand Island, NY, USA), 10% fetal calf serum (Gibco), 50,000 units penicillin (Huabei Pharmaceutical, Hebei, People's Republic of China), and 50,000 units streptomycin (Huabei) for use in establishment of a subcutaneously heterotopic transplantation HCC model in the rats. Approximately  $1 \times 10^7$  McA-RH7777 cells in 0.2 mL of phosphate-buffered saline solution (PBS) were injected into the fascia under the neck skin of 10 Buffalo rats (heterotopic transplantation HCC model), where tumors were grown to approximately 10 mm in diameter. All xenograft rats were then killed by intraperitoneal phenobarbital injection (100 mg/kg; Guangdong Bangmin Pharmaceutical, Guangdong, People's Republic of China), and tumors were harvested.

### Establishment of an orthotopic transplantation HCC model in the rats

An orthotopic transplantation HCC model was conducted as previously described.<sup>13</sup> Fresh harvested tumors were then implanted into the livers of Buffalo rats ( $n=70$ ). Briefly, rats were anesthetized by intraperitoneal injection of 50 mg/kg phenobarbital, left hepatic lobes were exposed by mid-line abdominal incision,  $1 \times 1$  mm tumor sections were implanted approximately 10 mm deep into shallow liver surface incisions, incisions were closed by pressure, and 3-0 polypropylene abdominal sutures were applied.

On day 15, magnetic resonance imaging (MRI) and laparotomy were performed under similar anesthesia, and rats exhibiting tumors on the liver surface were killed as a baseline ( $n=3$ ) or assigned to treatment with hepatic artery infusions of 0.1 mL normal saline ( $n=15$ , control group); 0.1 mL normal saline combined with daily intraperitoneal injection of ginsenoside Rg3 of purity  $>95\%$  (Jilin Yatai

Pharmaceutical, Jilin, People's Republic of China) dissolved in normal saline (1 mg/kg) (n=15, Rg3 group); embolization with 0.1 mL iodized oil (Guerbet, Villepinte, France) combined with daily intraperitoneal 0.1 mL normal saline injection (n=15, TAE group); or embolization with 0.1 mL iodized oil combined with daily intraperitoneal injection of ginsenoside Rg3 dissolved in normal saline (1 mg/kg) (n=15, TAE + Rg3 group).

## Transarterial embolization

TAE was conducted as previously described.<sup>14,15</sup> Briefly, the liver was retracted, the gastroduodenal artery was disconnected under a stereomicroscope (SMZ1500, Nikon, Tokyo, Japan), and the artery was cannulated in a retrograde manner with 2-F silastic tubing (SFM3-1050; SF Medical, Hudson, MA) by placing the tip prior to the bifurcation leading to the proper hepatic artery. Liquid iodized oil (0.1 mL) was used as an embolic agent by slow injection (~5 minutes) into the hepatic artery through the silastic tube.

## Sampling and assessment times

Animal weights were recorded for performance status at the beginning of each experiment and at every day thereafter. Tumor progression was monitored at 1, 2, 4, and 8 weeks after embolization combined with ginsenoside Rg3 treatment by MRI (1.5T, Siemens, Erlangen, Germany) and evaluated using Modified RECIST (mRECIST) assessment for HCC.<sup>16</sup> At 1, 2, and 4 weeks, three rats in each group were killed, and all remaining rats were killed at the end of 8 weeks. After rats were killed, tumors were excised. A 2×1×1 cm tumor tissue section was stored in formaldehyde and the remainder of the tumor was frozen in liquid nitrogen. Metastasis was determined by histological analysis with hematoxylin and eosin (HE) staining, using samples from the lung and lymph node tissues. Survival rate was analyzed and recorded at 8 weeks.

## Assessment of longest tumor diameter

A Magnetom Avanto 1.5T superconducting MRI (Siemens) with small animal coil was used to assess tumor diameter using the coronal plane MRI T1WI/T2WI, scanning with T1WI parameters of TR 400 ms, TE 9.1 ms, FOV 60 mm ×60 mm, slice thickness 2 mm, slice spacing 0.2 mm, average motivation for four times, flip angle 80°, and 192×192 pixels. T2WI parameters: TR 4350 ms, TE 86 ms, FOV 60 mm ×60 mm, slice thickness 2 mm, slice spacing 0.2 mm, average motivation for five times, flip angle 150°, and 192×192 pixels using a Syngo MR 2004 image processing workstation (Siemens). MRI scans were completed using maximum levels in order

to measure and record the longest diameter (in millimeters) of tumors.

## Immunohistochemical detection of CD31, VEGF, VEGF-R2, and phosphorylation of VEGF-R2

Immunohistochemistry (IHC) was performed on formalin-fixed, paraffin-embedded tumor tissue sections of 5 µm thickness. These specimens were dewaxed at 55°C for 30 minutes and washed in PBS three times for 3 minutes. Samples were then incubated with 3% hydrogen peroxide in methanol for 12 minutes at room temperature to block endogenous peroxidases. Sections were washed three times for 3 minutes with PBS (pH 7.5) and incubated for 20 minutes at room temperature in PBS supplemented with 1% normal goat serum (Gibco) and 5% normal horse serum (Gibco) as a protein-blocking solution. Slides were incubated with a polyclonal rabbit anti-CD31 (cluster of differentiation 31) (1:100 dilution), anti-VEGF (1:100 dilution), anti-VEGF receptor 2 (VEGF-R2) (1:100 dilution), or anti-phosphorylation of VEGF-R2 (1:100 dilution) (Abcam, Cambridge, MA, USA) at 4°C overnight, and rinsed three times for 3 minutes in PBS. Peroxidase-conjugated goat anti-rabbit secondary antibody (1:50 dilution; Cambridge Scientific Instruments, Cambridge, MA, USA) was then added for 1 hour at room temperature, and samples were washed and incubated with a stable diaminobenzidine substrate (Research Genetics, Huntsville, AL, USA). Staining was monitored under a bright-field microscope, and the reaction was stopped by washing sections with distilled water. Sections were counterstained with Gill's No 3 hematoxylin (Sigma-Aldrich, St Louis, MO, USA) and mounted with Universal Mount (Research Genetics) for 15 seconds.

## Microvessel density

Slides were divided evenly into 20 areas, and one field of 0.15 mm<sup>2</sup> was randomly examined by light microscopy (Olympus, Tokyo, Japan) at magnification ×400 in each of these areas by two independent pathologists blinded to study groupings as previously described.<sup>17</sup> CD31-positive endothelial cells or clearly separate clusters were counted as a single microvessel. The mean microvessel number per field was taken as the microvessel density (MVD) for each group. Images were analyzed with Image-Pro Plus 5.1 (Media Cybernetics, Rockville, MD, USA).

## ELISA detection of VEGF levels

Proteins were extracted from frozen tumor tissue using lysate buffer (1 mM phenylmethylsulfonyl fluoride (PMSF)

(Amresco, Solon, OH, USA), 20 mM Tris lysis buffer (pH 7.5), 150 mM NaCl, 1% Triton™ X-100 (Sigma-Aldrich), sodium pyrophosphate,  $\beta$ -glycerophosphate, ethylenediaminetetraacetic acid (EDTA),  $\text{Na}_3\text{VO}_4$ , and leupeptin (Beyotime). VEGF levels in tumor tissues were assayed using the enzyme-linked immunosorbent assay (ELISA) ChemiKine enzyme immunoassay kit (Chemicon International, Billerica, MA, USA), according to the manufacturer's instructions.

## Western blot detection of CD31, VEGF-R2, and phosphorylation of VEGF-R2

Proteins were extracted from frozen tumor tissue using lysis buffer (Beyotime Institute of Biotechnology, Jiangsu, People's Republic of China). Proteins were quantified using a bicinchoninic acid assay (BCA) protein assay kit (Beyotime). Equal amounts of protein were separated by 10% sodium dodecyl sulfate-polyacrylamide gel electrophoresis (SDS-PAGE) followed by electrophoretic transfer to nitrocellulose membranes (Merck Millipore, Billerica, MA, USA). Non-specific sites on each blot were blocked with 5% milk powder diluted in TBS with 0.05% Tween 20 (TBST) for 1.5 hours using polyclonal rabbit anti-CD31 (1:500 dilution), anti-VEGF-R2 (1:500 dilution), and anti-phosphorylation of VEGF-R2 (1:500 dilution) (Abcam). Glyceraldehyde 3-phosphate dehydrogenase (GAPDH) (Santa Cruz Biotechnology, Santa Cruz, CA, USA) was used as an internal control. The primary antibody was applied for 2 hours, and horseradish peroxidase-conjugated secondary antibodies (Jackson ImmunoResearch, West Grove, PA, USA) for 1 hour at room temperature. Proteins were detected using an enhanced chemiluminescence reagent (Pierce Protein Biology Products/Thermo Fisher Scientific, Rockford, IL, USA). Band intensity was quantified using an LAS-4000IR imaging system (Fujifilm, Tokyo, Japan).

## Statistical analysis

Data were reported as mean  $\pm$  standard deviation (SD) or medians (P25, P75) for quantitative data or as percentages, and analyzed with Statistical Package for the Social Sciences (SPSS) Version 13.0 (SPSS Inc., Chicago, IL, USA). Normally and non-normally-distributed data were compared with analysis of variance (ANOVA) with least significant difference (LSD) test for post hoc analysis or Kruskal–Wallis tests, respectively. Cochran–Mantel–Haenszel chi-square test was used to compare proportions between groups for categorical data. Tumor length and rat weight by times and groups were analyzed by repeated measures using ANOVA. Survival curves were constructed by the Kaplan–Meier method, and statistical significance was determined by log-rank test. *P*-values of less than 0.05 ( $P < 0.05$ ) were considered statistically significant.

## Results

### Outcomes of orthotopic transplantation HCC rat model construction and TAE

A total of 68 orthotopic transplantation HCC rats were successfully constructed, and the success rate of model development in the present study was 97.1% (68/70). Four rats died during the perioperative TAE, thus the success rate of surgery was 93.8% (61/65).

### Combined ginsenoside Rg3 and TAE reduced longest tumor diameter, body weight and metastasis in an orthotopic transplantation HCC rat model

No significant differences in the longest tumor diameter between TAE and TAE + Rg3 groups existed at week 4 ( $P > 0.05$ ), but with smaller tumors observed in TAE +

**Table 1** Longest tumor diameter and body weight

Time (week)	Control (n=6)		Rg3 (n=6)		TAE (n=6)		TAE + Rg3 (n=6)	
	Length (mm)	Weight (g)	Length (mm)	Weight (g)	Length (mm)	Weight (g)	Length (mm)	Weight (g)
0	9.3 $\pm$ 0.8	237.8 $\pm$ 6.9	8.7 $\pm$ 0.8	243.3 $\pm$ 8.7	9.2 $\pm$ 1.0	247.5 $\pm$ 6.5	9.5 $\pm$ 0.8	240.0 $\pm$ 6.1
1	13.0 $\pm$ 2.0	223.2 $\pm$ 4.8	9.5 $\pm$ 0.8*	239.8 $\pm$ 14.2*	10.8 $\pm$ 2.4*	227.0 $\pm$ 5.1	10.3 $\pm$ 0.8*	224.3 $\pm$ 12.6
2	17.3 $\pm$ 4.6	214.3 $\pm$ 9.5	12.2 $\pm$ 4.2	252.3 $\pm$ 12.4**	15.3 $\pm$ 6.8	236.2 $\pm$ 14.2*	11.2 $\pm$ 2.0*	240.3 $\pm$ 17.4*
4	23.7 $\pm$ 8.6	193.7 $\pm$ 12.9	15.3 $\pm$ 5.3*	274.2 $\pm$ 9.2**	19.5 $\pm$ 7.9	257.3 $\pm$ 10.3**	14.2 $\pm$ 3.4*	265.2 $\pm$ 16.7**
8	37.7 $\pm$ 16.6	129.7 $\pm$ 4.8	22.3 $\pm$ 5.2*	257.7 $\pm$ 16.0**	28.7 $\pm$ 13.4	213.8 $\pm$ 13.1**	19.5 $\pm$ 6.2*#	278.2 $\pm$ 28.9**##

**Notes:** Data are presented as mean  $\pm$  SD. Length is the longest tumor diameter. Weight is the body weight. Control group: treatment with hepatic artery infusions of 0.1 mL normal saline; Rg3 group: treatment with hepatic artery infusions of 0.1 mL normal saline combined with daily intraperitoneal injection of ginsenoside Rg3 dissolved in normal saline (1 mg/kg); TAE group: embolization with 0.1 mL iodized oil combined with daily intraperitoneal 0.1 mL normal saline injection; TAE + Rg3 group: embolization with 0.1 mL iodized oil combined with daily intraperitoneal injection of ginsenoside Rg3 dissolved in normal saline (1 mg/kg). \* $P < 0.05$ , \*\* $P < 0.001$  TAE + Rg3 group, TAE group, and Rg3 group versus control group; # $P < 0.05$ , ## $P < 0.01$  TAE + Rg3 group versus TAE group.

**Abbreviations:** TAE, transarterial embolization; SD, standard deviation.



**Table 2** Ginsenoside Rg3 reduced HCC metastasis rates after TAE following different treatments

	Intrahepatic metastasis rate (%)	Abdominal metastasis rate (%)	Distant metastasis rate (%)	Total metastasis rate (%)
Control (n=15)	10 (66.7%)	12 (80.0%)	5 (33.3%)	12 (80.0%)
Rg3 (n=15)	1 (6.7%)*	1 (6.7%)**	0 (0.0%)*	1 (6.7%)**
TAE (n=15)	7 (46.7%)	9 (60.0%)	4 (26.7%)	9 (60.0%)
TAE + Rg3 (n=15)	2 (13.3%)*	4 (26.7%)*	0 (0.0%)*#	4 (26.7%)*
$\chi^2$	6.667	188.0	29.4	1.067
P	0.010	0.000	0.000	0.302

**Notes:** \* $P < 0.05$ , \*\* $P < 0.001$  TAE + Rg3 group, TAE group, and Rg3 group versus control group; # $P < 0.05$  TAE + Rg3 group versus TAE group.

**Abbreviations:** HCC, hepatocellular carcinoma; TAE, transarterial embolization.

Rg3 rats at all time points. At week 8, the longest tumor diameter in TAE + Rg3 group was significantly shorter than that in the TAE group ( $P < 0.05$ ). Significant differences in the longest tumor diameters between control and Rg3 groups existed at all weeks except week 0 and week 2 ( $P < 0.05$ ), with smaller tumors observed in Rg3 rats at all time points (Table 1).

Significant differences in body weight were observed between control and Rg3 groups after 2 weeks of treatment (all  $P < 0.05$ ). Notably, at week 8 the body weight in the TAE + Rg3 group exceeded that in the TAE group ( $P < 0.05$ ) (Table 1).

TAE + Rg3 and Rg3 groups exhibited lower rates of intrahepatic and abdominal metastasis than other groups (all  $P < 0.05$ ), and no distant metastasis (Table 2). Total metastasis rates (%) in groups were as follows: control group 80.0% (12/15); Rg3 group 6.7% (1/15); TAE group 60.0% (9/15), and TAE + Rg3 group 26.7% (4/15).

### Combined ginsenoside Rg3 and TAE reduced MVD in an orthotopic transplantation HCC rat model

Significant differences in MVD (CD31-labeled MVD) were observed between control and Rg3 groups and TAE and TAE + Rg3 groups at all time points (all  $P < 0.05$ ).

At week 8, MVD in the TAE + Rg3 group was significantly reduced, compared with that in the TAE group ( $P < 0.01$ ) (Table 3 and Figure 1A and B). Western blot also confirmed that significant differences in CD31 expression were observed between control and Rg3 groups at all time points ( $P < 0.05$ ), and CD31 expression were significantly lower in the TAE + Rg3 group than those in the TAE group at 2 and 4 weeks ( $P < 0.05$ ) (Figure 1C).

### Combined ginsenoside Rg3 and TAE led to better overall survival in an orthotopic transplantation HCC rat model

Dyscrasia led to rat death in the control group (n=6), Rg3 group (n=1), TAE group (n=3), and TAE + Rg3 group (n=1) ( $P = 0.026$ ). Notably, overall survival was better in the TAE + Rg3 group compared with that in the TAE group (Figure 2).

### Ginsenoside Rg3 reduced hepatoma VEGF overexpression after TAE in an orthotopic transplantation HCC rat model

VEGF expression in tumor tissue was assessed by ELISA and IHC. ELISA revealed significant differences between Rg3 group and control group, and TAE group

**Table 3** Microvessel density

Time (week)	Control (n=15)		Rg3 (n=15)		TAE (n=15)		TAE + Rg3 (n=15)	
	MVD	WB (CD31)	MVD	WB (CD31)	MVD	WB (CD31)	MVD	WB (CD31)
0 (Baseline)	39.3±0.7							
1	39.1±0.3	1.12±0.22	29.4±1.2**	0.42±0.23*	42.0±0.7*	1.27±0.35	35.4±2.2*##	0.90±0.07
2	40.1±1.3	1.33±0.07	27.9±1.3**	0.56±0.10**	37.7±0.9	1.11±0.19	29.5±1.6*##	0.64±0.05*##
4	39.1±1.3	1.57±0.27	27.8±1.3**	0.37±0.13**	36.0±0.5*	1.15±0.17*	30.9±1.9*##	0.73±0.08*##
8	39.6±1.4	1.89±0.22	30.3±1.4**	0.52±0.21**	39.7±2.1	1.24±0.36**	32.3±2.1*##	1.11±0.25**

**Notes:** Data are presented as mean ± SD; MVD values represent the mean microvessel number per field (magnification ×400). \* $P < 0.05$ , \*\* $P < 0.01$  TAE + Rg3 group, TAE group, and Rg3 group versus control group; ## $P < 0.01$  TAE + Rg3 group versus TAE group.

**Abbreviations:** MVD, microvessel density; TAE, transarterial embolization; WB, Western blot; CD31, cluster of differentiation 31.

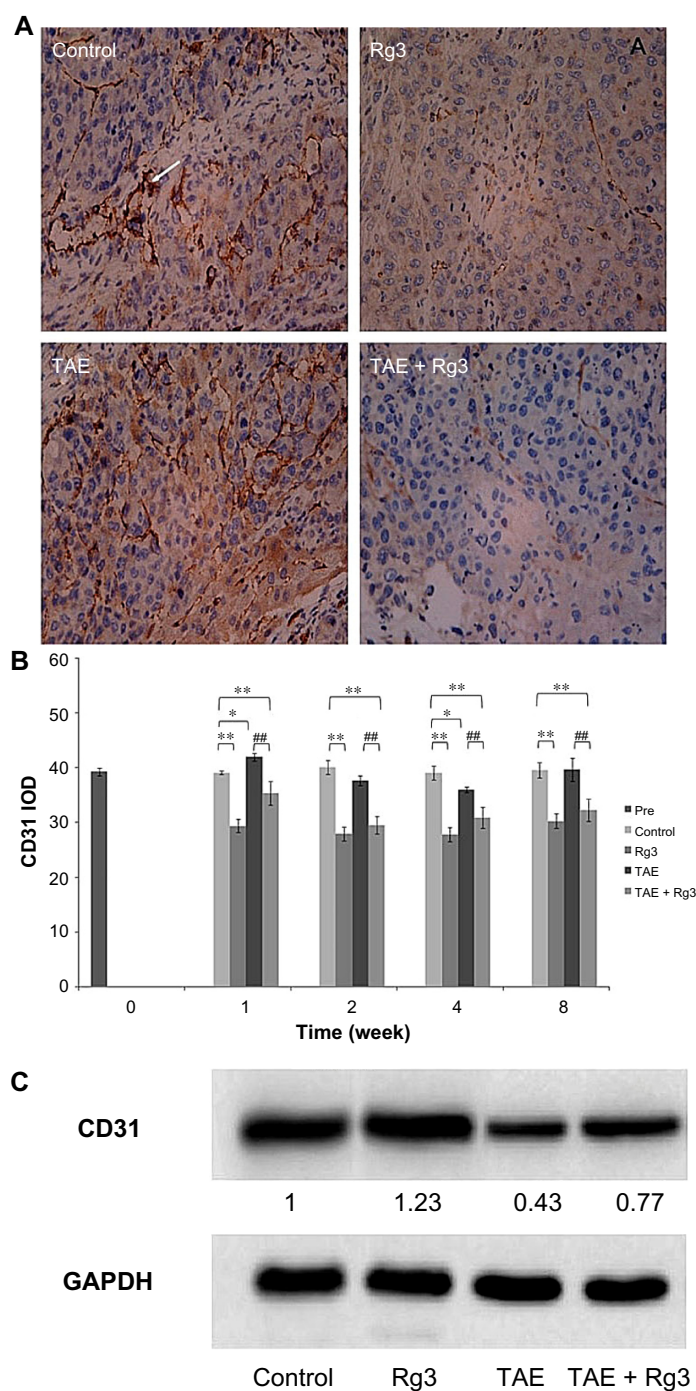


**Figure 1** Combined ginsenoside Rg3 and TAE reduced MVD in an orthotopic transplantation HCC rat model.

**Notes:** (A) Immunohistochemistry staining of hepatoma MVD labeled by CD31 at 4 weeks after TAE (magnification  $\times 400$ ). Arrow shows the CD31-positive cells. (B) Quantitative results of MVD. CD31-positive endothelial cells or clearly separate clusters were counted as single microvessels. Control group ( $n=3$ ), Rg3 group ( $n=3$ ), TAE group ( $n=3$ ), TAE + Rg3 group ( $n=3$ ). (C) CD31 expression was determined by Western blot. Protein expression was normalized to GAPDH. Control group ( $n=6$ ), Rg3 group ( $n=6$ ), TAE group ( $n=6$ ), TAE + Rg3 group ( $n=6$ ). These data represent the mean  $\pm$  SD of three independent experiments.  $*P<0.05$ ,  $**P<0.01$  TAE + Rg3 group, TAE group, and Rg3 group versus control group;  $###P<0.01$  TAE + Rg3 group versus TAE group.

**Abbreviations:** TAE, transarterial embolization; MVD, microvessel density; HCC, hepatocellular carcinoma; CD31, cluster of differentiation 31; IOD, immunohistochemical analysis of image gray integral optical density; GAPDH, glyceraldehyde 3-phosphate dehydrogenase; SD, standard deviation.

and TAE + Rg3 group, at all time intervals (all  $P<0.05$ ), with the exception of TAE and TAE + Rg3 at 8 weeks ( $P>0.05$ ) (Figure 3A). IHC staining confirmed VEGF

expression decreasing in the TAE + Rg3 group, compared with results of the TAE group, following 4 weeks of treatment (Figure 3B).

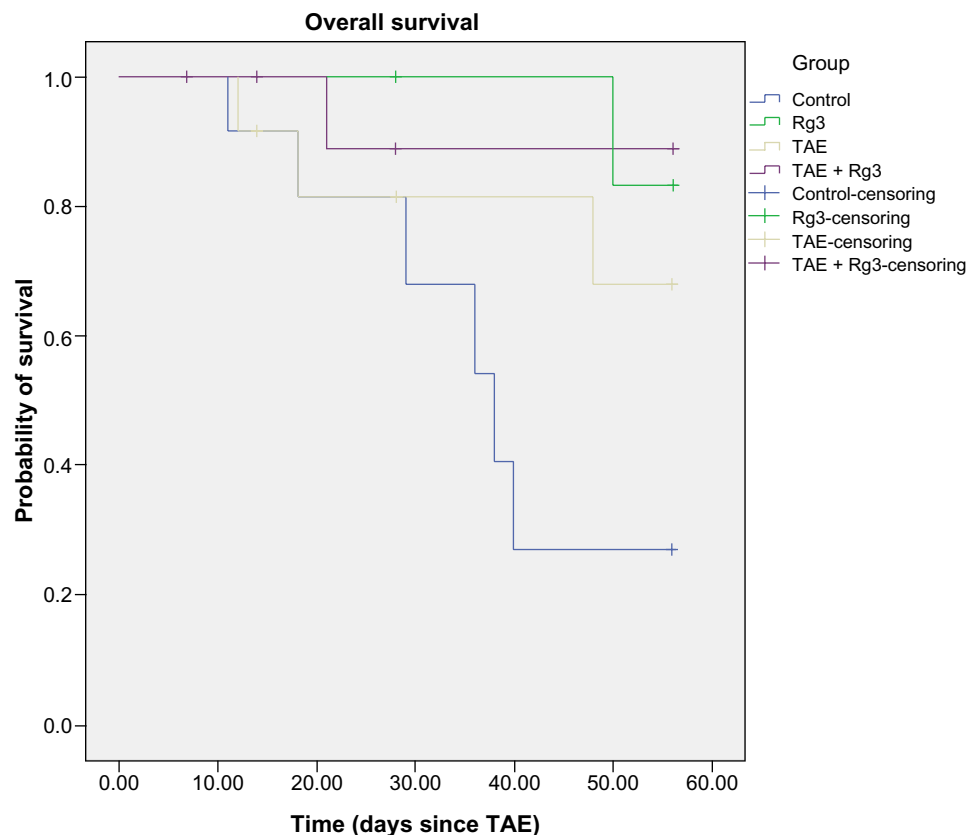


**Figure 2** Kaplan–Meier curves were plotted to determine overall survival rates of rats with hepatocellular carcinoma based on different treatments.

**Notes:** It can be seen that OS was better in the TAE + Rg3 group compared with that in the TAE group ( $P=0.303$ ). OS in the control group was worse than in the Rg3 group ( $P=0.017$ ), TAE group ( $P=0.152$ ), and TAE + Rg3 group ( $P=0.030$ ).

**Abbreviations:** TAE, transarterial embolization; OS, overall survival.

## Ginsenoside Rg3 reduced hepatoma VEGF-R2 expression and phosphorylation after TAE in an orthotopic transplantation HCC rat model

Expression and phosphorylation of VEGF-R2 were determined by Western blot (Figure 4A) and IHC (Figure 4B). Expression and phosphorylation of VEGF-R2 were significantly lower in the Rg3 group than those in the control group at all time points (all  $P<0.05$ ). Expression and phosphorylation of VEGF-R2 were significantly lower in the TAE + Rg3 group than those in the TAE group before 4 weeks of treatment (all  $P<0.05$ ); however, no significant difference was observed at 8 weeks ( $P>0.05$ ). IHC results also confirmed these findings (Figure 4B). Expression and phosphorylation of VEGF-R2 in the TAE + Rg3 group were significantly lower than those in the TAE group following 4 weeks of treatment.

## Discussion

Administration of combined TAE and ginsenoside Rg3 successfully reduced VEGF overexpression in HCC

tumors in rats. Furthermore, VEGF-R2 expression and phosphorylation, MVD, body weight and longest tumor diameter were lower in groups treated with ginsenoside Rg3. Better overall survival rates and reduced metastasis rates were observed in rats treated with combined TAE and ginsenoside Rg3, confirming the anti-angiogenic properties of Rg3. Thus, administration of ginsenoside Rg3 may be beneficial in combination with local TAE or TACE treatments, limiting potential hypoxia-induced tumor proliferation due to VEGF overexpression and angiogenesis.

Several mechanisms have been suggested for the anti-angiogenic quality of ginsenoside Rg3, including attenuation of the VEGF-dependent Akt/eNOS signaling pathways.<sup>11</sup> Another study showed that Rg3 treatment reduced hypoxia-induced phosphorylation of STAT3, ERK1/2, and JNK that downregulated VEGF expression in a dose-dependent manner.<sup>12</sup> Though the mechanism of Rg3 action remains unclear, the current study supports the theory that Rg3 acts on VEGF, thereby reducing the expression of a number of downstream signaling pathways involved in angiogenesis.

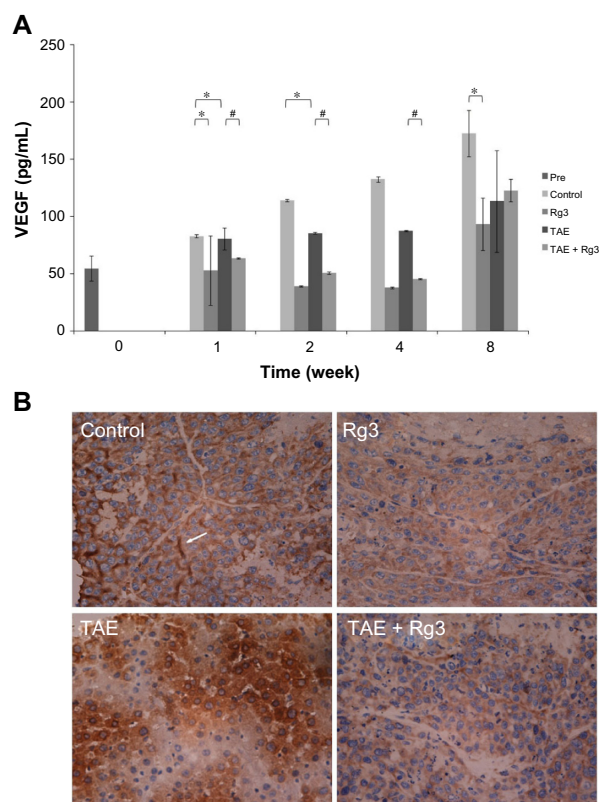


**Figure 3** Ginsenoside Rg3 reduced hepatoma VEGF overexpression after TAE in an orthotopic transplantation HCC rat model.

**Notes:** (A) VEGF expression was determined by ELISA. Data were expressed as mean  $\pm$  SD. \* $P < 0.05$ , TAE + Rg3 group, TAE group, and Rg3 group versus control group; # $P < 0.05$ , TAE + Rg3 group versus TAE group. Control group ( $n=3$ ), Rg3 group ( $n=3$ ), TAE group ( $n=3$ ), TAE + Rg3 group ( $n=3$ ). (B) Immunohistochemistry staining for VEGF expression after 4 weeks of treatment (magnification  $\times 400$ ). Control group ( $n=3$ ), Rg3 group ( $n=3$ ), TAE group ( $n=3$ ), TAE + Rg3 group ( $n=3$ ).

**Abbreviations:** TAE, transarterial embolization; HCC, hepatocellular carcinoma; ELISA, enzyme-linked immunosorbent assay; SD, standard deviation; VEGF, vascular endothelial growth factor.

Previous studies have explored the potential for combining Rg3 with local treatments to reduce cancer recurrence and metastasis. Zhang et al<sup>18</sup> reported that Rg3 had anti-angiogenic effects when combined with capecitabine chemotherapy for breast cancer treatment. In mice, these results demonstrated both lower toxicity and reduced susceptibility to drug resistance.<sup>19</sup> Liu et al<sup>20</sup> demonstrated similar results by combining gemcitabine with Rg3 in lung cancer treatment, resulting in improved overall survival and quality of life in tumor-bearing mice. Thus, this study is consistent with previous work indicating that Rg3 may be effectively combined with local treatments to increase survival and reduce recurrence, though this is the first work to report these findings for cancer of the liver.

In addition to improving survival, the current findings also reported that combined TAE and Rg3 treatment reduce metastasis rates dramatically. Metastasis is known to be

caused, in part, by activation of Rac, a GTPase of the Rho family.<sup>1</sup> It has been demonstrated that Rac activation has a strong correlation with expression of VEGF<sup>21</sup>, which may provide a basis for reduced metastasis following Rg3 treatments that lower the overexpression of VEGF typical in HCC tumor cells. These findings are consistent with previous reports that the saponins ginsenoside-Rb2, 20(R)-ginsenoside-Rg3, and 20(S)-ginsenoside-Rg3 reduce metastasis in both colon and lung cancer.<sup>22</sup> Similarly, it has been reported that ginsenoside Rg3 can significantly inhibit the metastasis of ovarian cancer, a process that Xu et al<sup>23</sup> speculated was related to the inhibitory effect of Rg3 on the invasive ability and MMP-9 expression of SKOV-3 cells. Thus, Rg3 may act to reduce metastatic action of HCC by both limiting angiogenesis and reducing the invasive ability of remaining tumor cells after local TAE treatment, as demonstrated in the current study.

It is important to note that, while consistent with previous results, HCC tumors have unique pathomorphologic characteristics, particularly in the case of very small HCCs ( $< 2$  cm) that may cause treatment outcomes to vary between HCC and other cancer types.<sup>24</sup> Thus, this research should be further considered in cases where tumors are small and indistinct as well as in larger tumors with very poor margins. As VEGF upregulation, as well as a number of other processes associated with metastasis and recurrence, is centralized in the tumor margin<sup>1</sup>, it is important to consider the effects that varied tumor characteristics may have on the outcomes of this treatment strategy. Furthermore, this treatment (TAE + Rg3) is currently pending preliminary clinical investigation by the authors in order to determine the actual effects of treatment in human HCC patients.

Limitations to the study exist. Substantive statistical analysis was limited by relatively small sample sizes. Our exploratory study yielded some promising and desired results, but other results were inconclusive or contradictory. Further confirmation of this study is needed, and future research will find our data useful.

The current study provided novel preliminary evidence that ginsenoside Rg3 combined with conventional TAE treatment may effectively limit HCC tumor progression, reduce metastasis, and increase overall survival. Ginsenoside Rg3 combined with TAE effectively reduced overexpression of VEGF, a typical feature of highly vascular HCC tumors, thereby downregulating a number of downstream processes related to angiogenesis and tumor proliferation. Therefore, ginsenoside Rg3 combined with TAE is an interesting target for further clinical study as a combined agent for HCC treatment.



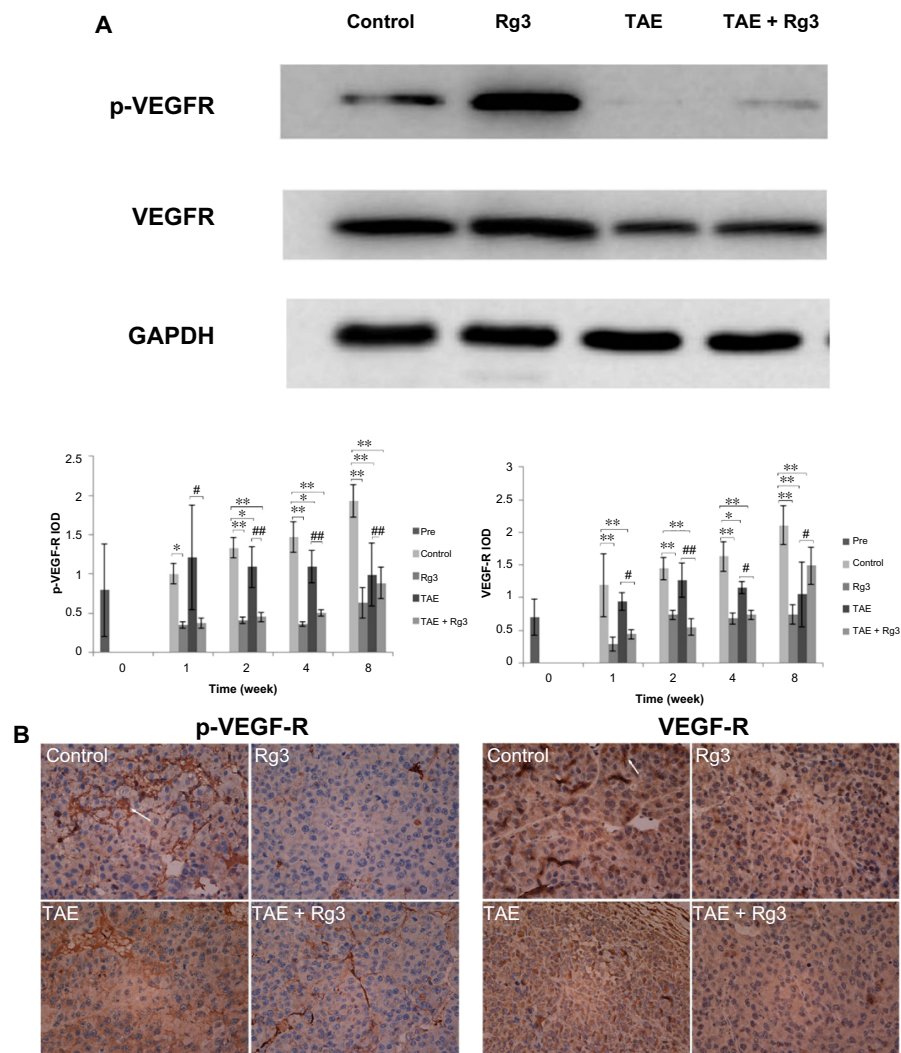


**Figure 4** Ginsenoside Rg3 reduced hepatoma VEGF-R2 expression and phosphorylation after TAE in an orthotopic transplantation HCC rat model.

**Notes:** (A) VEGF-R2 expression and phosphorylation were determined by Western blot. Protein expression was normalized to GAPDH. The data represent the mean  $\pm$  SD of three independent experiments. \* $P < 0.05$ , \*\* $P < 0.01$  TAE + Rg3 group, TAE group, and Rg3 group versus control group; # $P < 0.05$ , ## $P < 0.01$  TAE + Rg3 group versus TAE group. Control group ( $n=3$ ), Rg3 group ( $n=3$ ), TAE group ( $n=3$ ), TAE + Rg3 group ( $n=3$ ). (B) Immunohistochemistry staining for VEGF-R2 expression and phosphorylation after 4 weeks of treatment (magnification  $\times 400$ ). Arrows show the VEGF-R2 or VEGF-R2 phosphorylation-positive cells. Control group ( $n=3$ ), Rg3 group ( $n=3$ ), TAE group ( $n=3$ ), TAE + Rg3 group ( $n=3$ ).

**Abbreviations:** VEGF-R2, vascular endothelial growth factor receptor 2; TAE, transarterial embolization; IOD, immunohistochemical analysis of image gray integral optical density; GAPDH, glyceraldehyde 3-phosphate dehydrogenase; SD, standard deviation.

## Author contributions

All authors contributed to laboratory studies, critically reviewed the manuscript, and gave final approval of the paper to be published. Jianhua Wang participated in all aspects of the study. Bo Zhou contributed to study integrity and literature searching. Zhiping Yan contributed to study concepts and design. Bo Zhou and Zhiping Yan contributed to data acquisition, analysis, and interpretation, and preparation of the final manuscript.

## Disclosure

The authors report no conflicts of interest in this work.

## References

1. Strelbe BM, Dufour JF. Combined approach to hepatocellular carcinoma: a new treatment concept for nonresectable disease. *Expert Rev Anticancer Ther.* 2008;8:1743–1749.
2. Jemal A, Bray F, Center MM, Ferlay J, Ward E, Forman D. Global cancer statistics. *CA Cancer J Clin.* 2011;61(2):69–90.
3. Marelli L, Stigliano R, Triantos C, et al. Transarterial therapy for hepatocellular carcinoma: which technique is more effective? A systematic review of cohort and randomized studies. *Cardiovasc Intervent Radiol.* 2007;30(1):6–25.
4. Kim YB, Park YN, Park C. Increased proliferation activities of vascular endothelial cells and tumour cells in residual hepatocellular carcinoma following transcatheter arterial embolization. *Histopathology.* 2001;38(2):160–166.
5. Gomaa AI, Khan SA, Toledano MB, Waked I, Taylor–Robinson SD. Hepatocellular carcinoma: epidemiology, risk factors and pathogenesis. *World J Gastroenterol.* 2008;14(27):4300–4308.

6. Parkin DM, Bray F, Ferlay J, Pisani P. Global cancer statistics, 2002. *CA Cancer J Clin*. 2005;55(2):74–108.
7. An FQ, Matsuda M, Fujii H, Matsumoto Y. Expression of vascular endothelial growth factor in surgical specimens of hepatocellular carcinoma. *J Cancer Res Clin Oncol*. 2000;126 (3):153–160.
8. Cammà C, Schepis F, Orlando A, et al. Transarterial chemoembolization for unresectable hepatocellular carcinoma: meta-analysis of randomized controlled trials. *Radiology*. 2002;224(1):47–54.
9. Llovet JM, Real MI, Montana X, et al. Arterial embolisation or chemoembolisation versus symptomatic treatment in patients with unresectable hepatocellular carcinoma: a randomised controlled trial. *Lancet*. 2002;359(9319):1734–1739.
10. Llovet JM, Ricci S, Mazzaferro V, et al. Sorafenib in advanced hepatocellular carcinoma. *N Engl J Med*. 2008;359(4):378–390.
11. Kim JW, Jung SY, Kwon YH, et al. Ginsenoside Rg3 inhibits endothelial progenitor cell differentiation through attenuation of VEGF-dependent Akt/eNOS signaling. *Phytother Res*. 2012;26(9):1286–1293.
12. Chen QJ, Zhang MZ, Wang LX. Ginsenoside Rg3 inhibits hypoxia-induced VEGF expression in human cancer cells. *Cell Physiol Biochem*. 2010;26(6):849–858.
13. Guo Y, Klein R, Omary RA, Yang GY, Larson AC. Highly malignant intra-hepatic metastatic hepatocellular carcinoma in rats. *Am J Transl Res*. 2010;3(1):114–120.
14. Kan Z, Ivancev K, Hagerstrand I, Chuang VP, Lunderquist A. In vivo microscopy of the liver after injection of Lipiodol into the hepatic artery and portal vein in the rat. *Acta Radiol*. 1989;30(4):419–425.
15. Kan Z, Sato M, Ivancev K, et al. Distribution and effect of iodized poppyseed oil in the liver after hepatic artery embolization: experimental study in several animal species. *Radiology*. 1993;186(3):861–866.
16. Eisenhauer EA, Therasse P, Bogaerts J, et al. New response evaluation criteria in solid tumours: revised RECIST guideline (version 1.1). *Eur J Cancer*. 2009;45(2):228–247.
17. Weidner N. Current pathologic methods for measuring intratumoral microvessel density within breast carcinoma and other solid tumors. *Breast Cancer Res Treat*. 1995;36(2):169–180.
18. Zhang Q, Kang X, Yang B, Wang J, Yang F. Antiangiogenic effect of capecitabine combined with ginsenoside Rg3 on breast cancer in mice. *Cancer Biother Radiopharm*. 2008;23(5):647–653.
19. Mattern J, Koomagi R, Volm M. Association of vascular endothelial growth factor expression with intratumoral microvessel density and tumour cell proliferation in human epidermoid lung carcinoma. *Br J Cancer*. 1996;73(7):931–934.
20. Liu TG, Huang Y, Cui DD, et al. Inhibitory effect of ginsenoside Rg3 combined with gemcitabine on angiogenesis and growth of lung cancer in mice. *BMC Cancer*. 2009;9:250.
21. Xiong ZP, Yang SR, Liang ZY, et al. Association between vascular endothelial growth factor and metastasis after transcatheter arterial chemoembolization in patients with hepatocellular carcinoma. *Hepatobiliary Pancreat Dis Int*. 2004;3(3):386–390.
22. Mochizuki M, Yoo YC, Matsuzawa K. Inhibitory effect of tumor metastasis in mice by saponins, ginsenoside-Rb2, 20(R)- and 20(S)-ginsenoside-Rg3, of red ginseng. *Biol Pharm Bull*. 1995;18(9):1197–1202.
23. Xu TM, Cui MH, Xin Y, et al. Inhibitory effect of ginsenoside Rg3 on ovarian cancer metastasis. *Chin Med J (Engl)*. 2008;121(15):1394–1397.
24. Nakashima O, Sugihara S, Kage M, Kojiro M. Pathomorphologic characteristics of small hepatocellular carcinoma: a special reference to small hepatocellular carcinoma with indistinct margins. *Hepatology*. 1995;22(1):101–105.

## OncoTargets and Therapy

### Publish your work in this journal

OncoTargets and Therapy is an international, peer-reviewed, open access journal focusing on the pathological basis of all cancers, potential targets for therapy and treatment protocols employed to improve the management of cancer patients. The journal also focuses on the impact of management programs and new therapeutic agents and protocols on

Submit your manuscript here: <http://www.dovepress.com/oncotargets-and-therapy-journal>

Dovepress

patient perspectives such as quality of life, adherence and satisfaction. The manuscript management system is completely online and includes a very quick and fair peer-review system, which is all easy to use. Visit <http://www.dovepress.com/testimonials.php> to read real quotes from published authors.